

# CHAPTER I

## INTRODUCTION

### 1.1 Porphyrins

The porphyrins are a class of naturally occurring macrocyclic aromatic compounds and are ubiquitous in our world. The word “porphyrin” is derived from the Greek “porphura” meaning purple [1]. On account of their large  $\pi$ -conjugated system, all porphyrins are intensely colored. As such, they have been called the pigments and the colors of life. This auspicious designation reflects their importance in numerous biological functions. Indeed, life as we understand it relies on the full range of biological processes that are either performed by or catalyzed by porphyrin-containing substances. Complexes of many metals with various porphyrins play a key role in biological activities as for instance iron complexes in the haemoprotein and cytochrome C, magnesium complexes in the chlorophylls, and a cobalt complex in Vitamin B<sub>12</sub> (Figure 1.1).

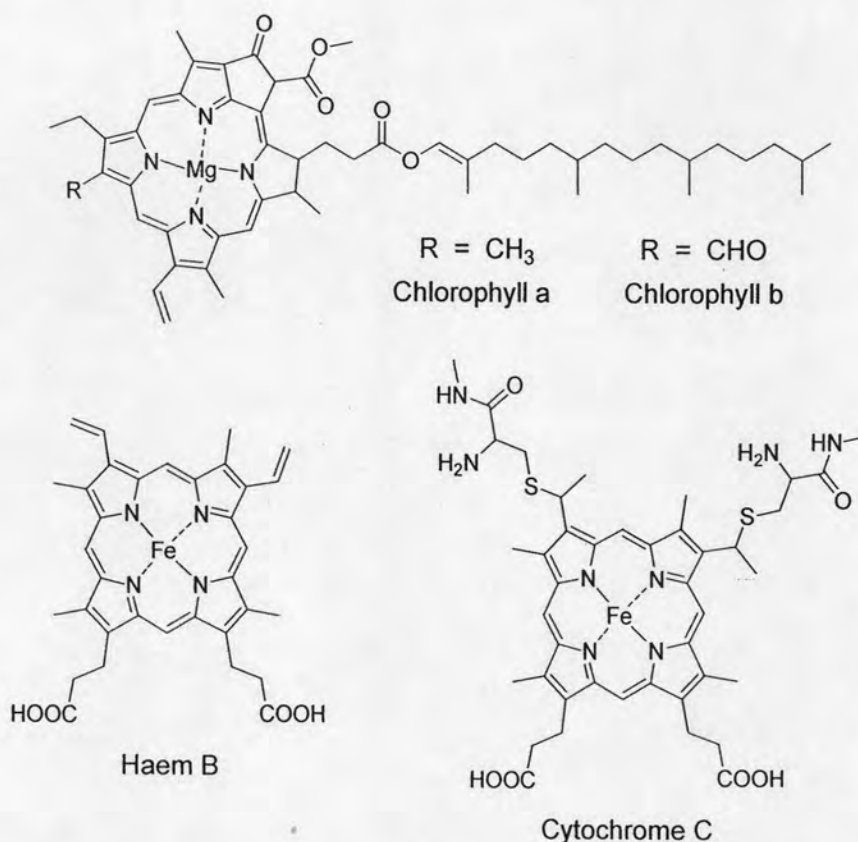


Figure 1.1 Structures of naturally occurring porphyrin derivatives

In haemoglobins and myoglobins, haem is the prosthetic group which is responsible for oxygen transport and storage in living tissues. Furthermore, haem can also be found in cytochrome C to function in an array of reactions as a single electron carrier in the electron transport chain and as a catalyst for redox reactions [2]. The reduction of one of the pyrrole units on the porphyrin ring leads to the formation of a class of porphyrin derivatives called “Chlorins”. Chlorophylls are chlorin pigments which are structurally similar to and produced through the same metabolic pathway as haem. They are found abundantly in green plants as photosynthetic reaction centers which convert light energy into chemical energy while producing oxygen along the way [3].

Not surprisingly, therefore, these molecules remain of fundamental interest to chemists and biochemists. Indeed, they continue to be intensely investigated by researchers worldwide. In recent years, a large number of porphyrin derivatives have been synthesized and studied to determine and mimic the electron or energy transfer mechanisms of natural photosynthetic reaction centers and light harvesting complexes [4]. In addition, porphyrin derivatives have been widely proven hitherto in relation to photocatalysts [5], photodynamic therapeutic agents [6], optical sensors [7,8], organic semiconductors [9], and optoelectronic devices such as photovoltaic cells [10], organic light emitting diodes [11], photonic molecular switches [12], and nonlinear optical (NLO) materials [13,14].

## 1.2 Structure and Nomenclature of Porphyrins

Porphyrin is a tetrapyrrolic macrocyclic system consisting of four pyrrole units linked together by four methine bridges between the  $\alpha$ -positions of the five-membered pyrrole rings. The nomenclature based on the numbering system which is commonly used in porphyrin chemistry was created by Hans Fischer. Along with this simple numbering system, the pyrrolic positions are numbered from 1 to 8 and the bridging positions named  $\alpha$ ,  $\beta$ ,  $\gamma$ , and  $\delta$ . Fischer's system is relative to a very large number of trivial names and a numeration scheme for the unsubstituted porphyrin ring system, which is simple but incomplete, is used as shown in **Figure 1.2**. The availability of a more systematic nomenclature has helped interdisciplinary communication, and has considerably diminished the need for new trivial names. These recommendations provide for naming porphyrins, hydroporphyrins, ring contracted or expanded

porphyrins, porphyrins fused with other rings, skeletally replaced porphyrins and porphyrin-metal coordination complexes together with corresponding linear arrangements of three and four pyrrole rings. The application of these recommendations permits these substances to be named more systematically using fewer trivial names. The inability of the Fischer's system to name the large number of synthetic and newly isolated porphyrins led to the adoption of a systematic nomenclature based on 1-24 numbering system (**Figure 1.2**) which is developed by a joint commission on biochemical nomenclature, consisting of the International Union of Pure and Applied Chemistry (IUPAC) and the International Union of Biochemistry (IUB).

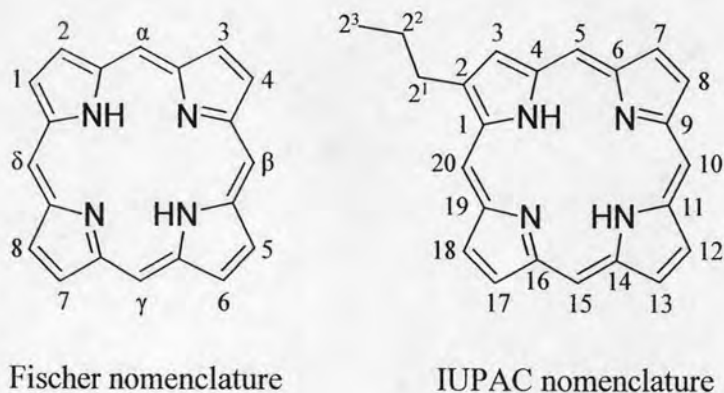


**Figure 1.2** Structure and nomenclature of porphyrin in Fischer's system relative to IUPAC system

The 1-24 numbering system is adopted for the porphyrin nucleus. The 2, 3, 7, 8, 12, 13, 17, and 18 positions have commonly been referred to generically as " $\beta$ -positions". Similarly, the 1, 4, 6, 9, 11, 14, 16, and 19 positions have been referred to generically as " $\alpha$ -positions", while the 5, 10, 15, and 20 positions have been referred to generically as "*meso*-positions". However, in order to avoid possible ambiguity with stereochemical designations, the use of these generic terms is discouraged.

### 1.3 Synthetic Strategies to Porphyrins

In fact, porphyrins have been synthesized by various routes depending on the different substituents on the porphyrin ring. The routes employed generally become more elaborate as the number of different substituents increases. However, all of the synthetic routes of porphyrins can be divided in four types based on the number of

pyrrolic subunits in starting materials: monopyrrolic, dipyrrolic, tripyrrolic, and tetrapyrrolic intermediates.

### 1.3.1 Synthesis of Porphyrins *via* Monopyrrole Tetramerization

Monopyrrole tetramerization is the simplest synthetic strategy to porphyrins which can only produce a structurally unique product if the 3- and 4-substituents in the monopyrrole are identical. Several methods relying on this strategy were discovered and developed in many ways.

The most easily synthesized porphyrin is tetraphenylporphyrin (TPP) that simply needs to react pyrrole with benzaldehyde under acidic conditions. The first route was reported by Rothmund, who preferred to carry out the reaction in sealed glass tubes at high temperature [15].

Subsequently, a modification by Adler, Longo and their colleagues involving use of refluxed propionic acid instead of sealed tubes chemistry reproducibly obtained a 20-25% yield of TPP [16]. This trivial procedure concerned the addition of equimolar amounts of pyrrole and benzaldehyde to refluxed propionic acid; after heating for about one half hour, the mixture was allowed to cool and the product TPP was filtered off (**Figure 1.3**). This procedure has been widely used when large amounts of porphyrins are needed and the corresponding aldehydes are able to survive under the condition of refluxed propionic acid.

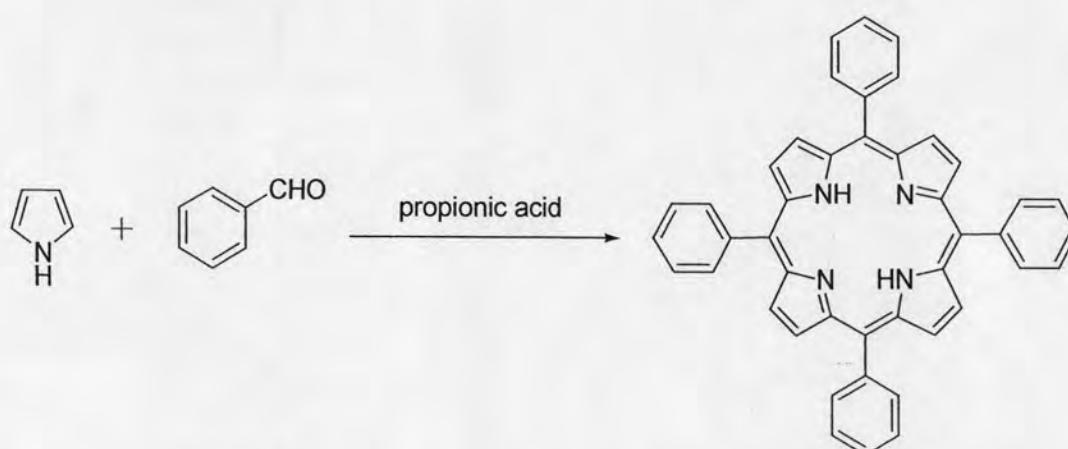


**Figure 1.3** Synthesis of tetraphenylporphyrin (TPP) from monopyrrole using Adler-Longo's procedure



The synthesis was finally optimized by Lindsey's group which showed the mild condition reactions and excellent yields of a wide variety of tetraarylporphyrins [17]. The porphyrins can be obtained using a high dilution two step reaction of arylaldehydes and pyrrole. In the first step, the acid-catalyzed condensation reaction is carried out in the presence of trace acid catalyst, usually  $\text{BF}_3 \cdot \text{OEt}_2$  or TFA, to form tetraarylporphyrinogen. In the second step of the reaction, the initial porphyrinogen intermediate is irreversibly oxidized by a quinone derivative such as 2,3-dichloro-5,6-dicyanobenzoquinone (DDQ) to afford the desired tetraarylporphyrin (**Figure 1.4**).

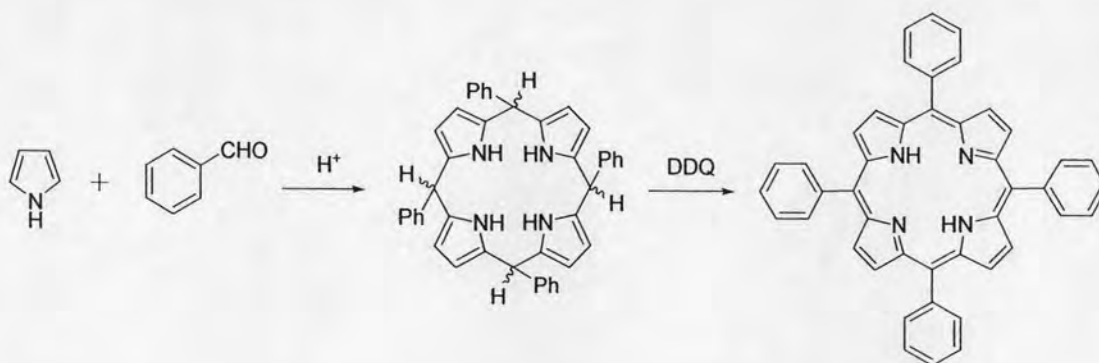


**Figure 1.4** Synthesis of tetraphenylporphyrin (TPP) from monopyrrole using Lindsey's procedure

Most naturally occurring porphyrins do not contain *meso*-substituents, and there are certainly none that possess four such substituents. Thus, octaethylporphyrin (OEP) has been favored as a model for natural porphyrins more than has TPP. There are two main routes to synthesize the prototypical OEP as illustrated in **Figure 1.5**. Firstly, tetramerization of 3,4-diethylpyrrole with formaldehyde in the presence of acid catalyst afforded OEP in satisfactory yield (55-75%) [18]. Secondly, tetramerization of pyrrole bearing  $\text{CH}_2\text{-R}$  substituents, which was prepared by Mannich reaction of 3,4-diethylpyrrole with formaldehyde and dimethylamine, gave acceptable yields of porphyrin when "R" group is a good leaving group. It is because the methylene carbon will eventually be the source of the interpyrrolic carbons of the product [19].

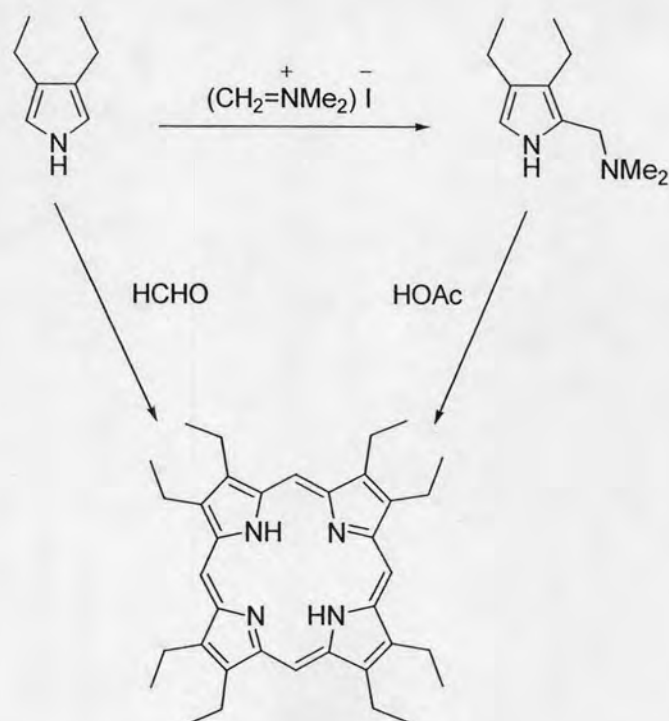


**Figure 1.5** Synthesis of octaethylporphyrin (OEP) from monopyrrole

Monopyrrole tetramerization works best for pyrroles with identical 3- and 4-substituents. If the 3- and 4-substituents on the monopyrrole reactant are not identical, mixtures will usually result due to acid-catalyzed pyrrole ring scrambling reactions.

While easy to synthesize, these symmetrical porphyrins suffer in that there is no provision to be able to control functionalization at individual *meso*-positions, severely limiting factor in the quest to form large covalently bonded arrays. It is possible to synthesize unsymmetrically substituted porphyrins *via* mixed aldehyde condensations. If a mixture of two different aldehyde starting materials is employed, then a statistical mixture of products is obtained. The desired porphyrin is then removed by extensive chromatography. The disadvantages here are that yields are lower by virtue of the statistical outcome of the reaction and the separation procedures can be troublesome, particularly if the reactions are carried out on a significant scale.

### 1.3.2 Synthesis of Porphyrins from Dipyrromethanes

Alternative approaches for the synthesis of substituted porphyrins have been devised in which dipyrrolic starting materials are combined to form tetrapyrrole compounds. Dipyrromethanes are the key intermediates in the synthesis of porphyrins

by the MacDonald [2+2] approach. Such intermediates can be synthesized using fairly straightforward methods. A number of stepwise syntheses of symmetrically and unsymmetrically substituted dipyrromethanes have been developed, while more direct routes have employed one-flask condensations of pyrrole and the desired aldehyde [20].

Condensation of two dipyrromethanes with appropriate bridging carbons will result in porphyrins. For instance, two unsymmetrically substituted dipyrromethanes can be condensed in two orientations to obtain two different porphyrins as shown in **Figure 1.6**.

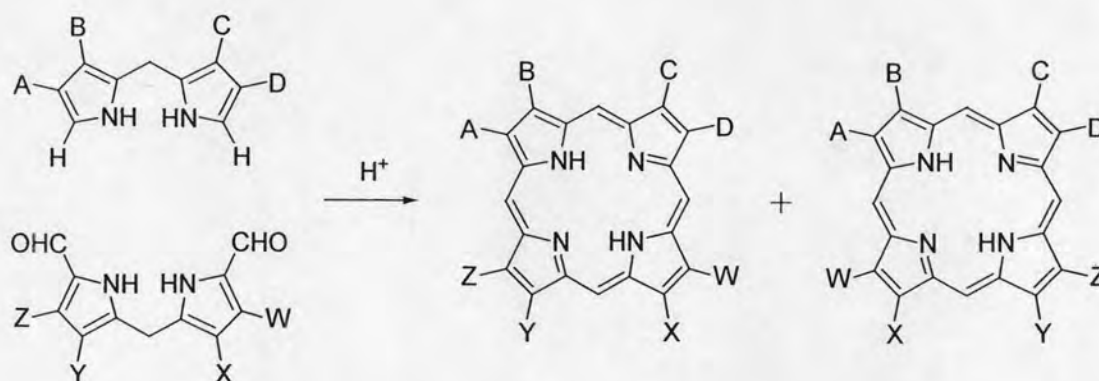


**Figure 1.6** Synthesis of porphyrins from two unsymmetrically substituted dipyrromethanes using the MacDonald [2+2] approach

These symmetry complications in the synthesis of porphyrin involving an A-B or C-D dipyrromethane can be avoided if the A-B or C-D dipyrromethane unit is symmetrical about its interpyrrolic carbon atom. Thus, MacDonald and co-workers generically exhibited that a 1,9-diformyldipyrromethane reacted with a 1,9-di-unsubstituted dipyrromethane containing hydriodic acid catalyst to afford pure porphyrin in over 60% yield (**Figure 1.7**) [21].

In addition to the MacDonald [2+2] approach, another [2+2] method involves the acid-catalyzed condensation of 1,9-di-unfunctionalized dipyrromethanes with aldehydes to form porphyrinogens, which are then chemically oxidized to give porphyrins (**Figure 1.8**) [22].

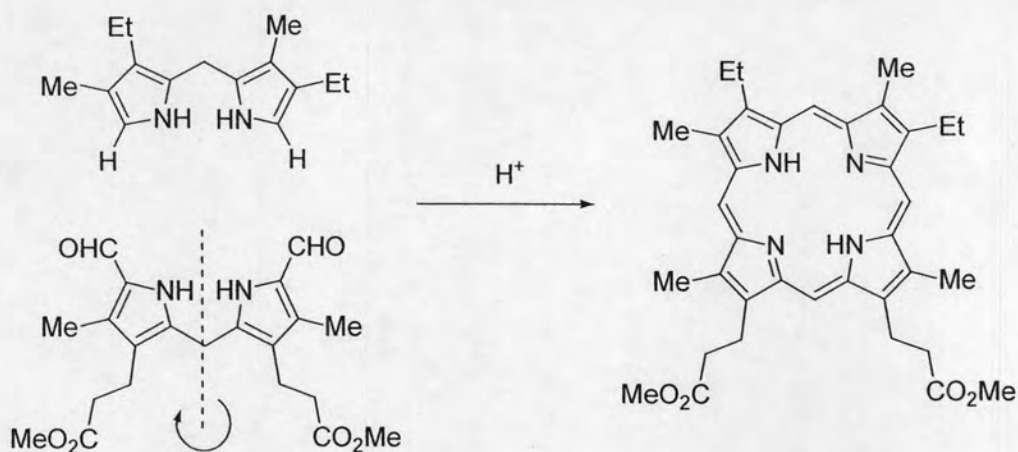


**Figure 1.7** Synthesis of porphyrin from symmetrically substituted dipyrromethane using the MacDonald [2+2] approach

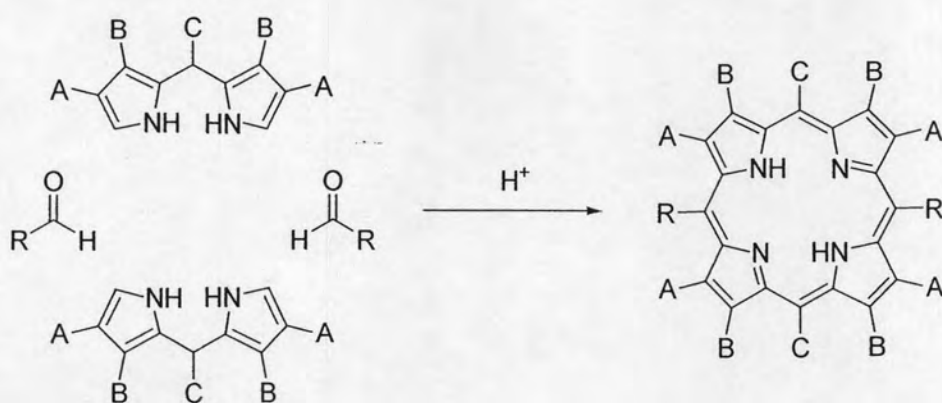


**Figure 1.8** Synthesis of porphyrin from symmetrically substituted 1,9-di-unfunctionalized dipyrromethanes and aldehydes

This methodology is considerably more versatile for a wide variety of porphyrins, especially unsymmetrically substituted porphyrins as it is frequently higher yielding and allows control over substitution at the *meso*-positions. There is however a trade off, the time and resources required to make the precursor dipyrromethane molecules.



### 1.3.3 Synthesis of Porphyrins from Tripyrranes

Tripyrranes play an important role in the preparation of porphyrins by the [3+1] route. An opened chain tripyrrane can be reacted with a 2,5-difunctionalized monopyrrole bearing the two bridging carbon atoms to form a porphyrin as illustrated in **Figure 1.9**. Using the [3+1] protocol permits one to efficiently synthesize a porphyrin in which the required functional handle group is situated on the monopyrrole component to be inserted at the final stage. However, the [3+1] route has symmetry limitations because the terminal rings of the tripyrrane are usually identical.

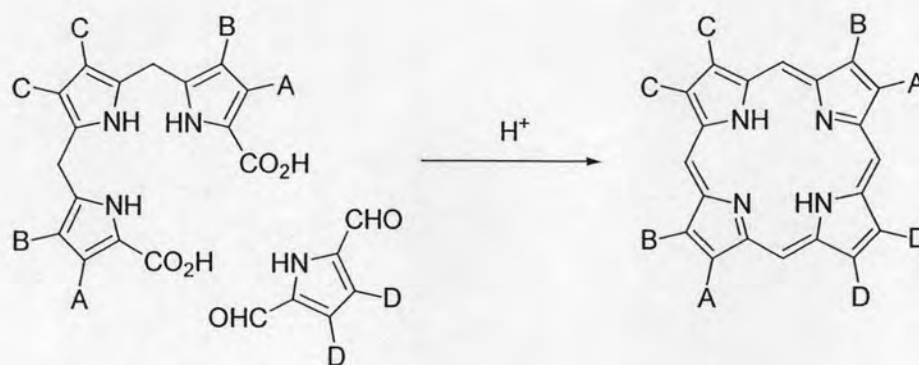


**Figure 1.9** Synthesis of porphyrin from tripyrrane and monopyrrole using the [3+1] approach

### 1.3.4 Synthesis of Porphyrins from Tetrapyrrolic Intermediates

The synthesis of a porphyrin with a completely unsymmetrical array of substituents must progress through opened chain tetrapyrrolic intermediates. The opened chain tetrapyrrole of choice have been shown to be 1,19-dimethyl-a,c-biladiene salt as depicted in **Figure 1.10**. Symmetrically substituted 1,19-dimethyl-a,c-biladiene could be synthesized by condensation of dipyrromethane-1,9-dicarboxylic acids with two equivalents of a 2-formyl-5-methylpyrrole. The cyclization of the a,c-biladiene has involved use of copper(II) chloride or acetate to give porphyrin copper complex. Demetallation then afforded the metal free porphyrin [23].

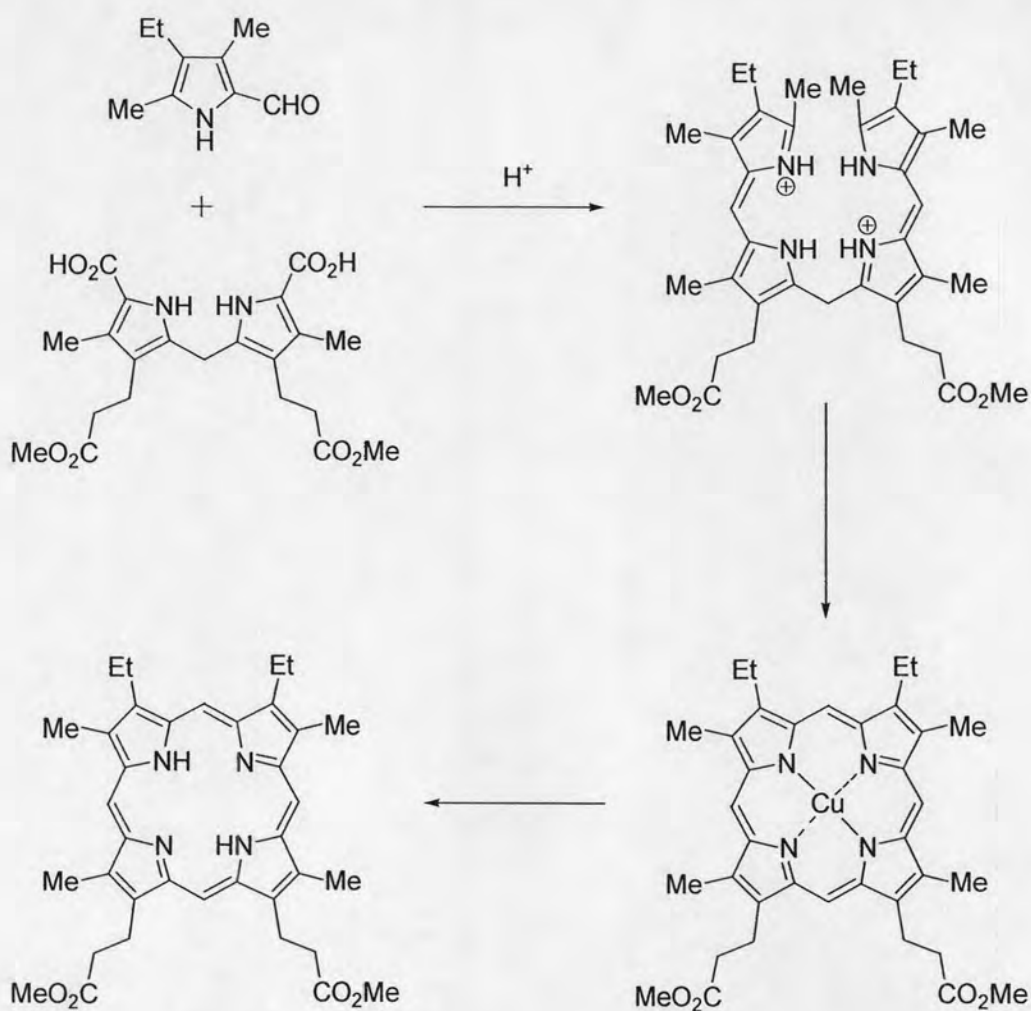


**Figure 1.10** Synthesis of porphyrin from tetrapyrrolic intermediate

#### 1.4 Reactivity Profiles of Porphyrins

In porphyrins, there are a total of 22 conjugated  $\pi$ -electrons, only 18 of which are included in any conjugation pathway that causes these molecules to have aromatic characteristics. Two possible conjugation pathways have been proposed based on aromatic ring current and bond distance data (**Figure 1.11**) [24]. One is an inner 18-electron, 16-orbital subfragment (a structure similar to [16]-annulene) and the other is an outer 18-electron, 18-orbital subfragment (a structure similar to [18]-annulene). A number of electronic structure calculations, X-ray crystallographic, and aromatic ring current studies support both the [16]-annulene and 18-annulene structure as the predominant porphyrin conjugative pathways [25]. The [16]-annulene structure is a  $\pi$ -excessive subfragment, whereas the [18]-annulene structure is a  $\pi$ -deficient subfragment. Moreover, the analysis of electron density on the various carbon atoms

of the two subfragments show that in both the cases, the *meso*-positions are electron deficient and the  $\beta$ -positions are electron excessive [25].

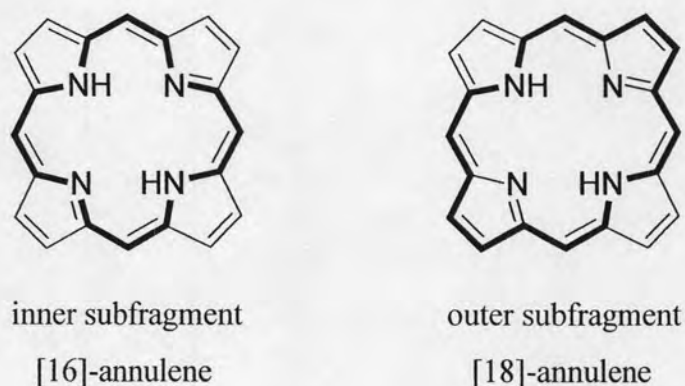


**Figure 1.11** The inner and outer aromatic subfragments of the porphyrin skeleton

In the case of the [18]-annulene structure, the tautomeric forms with *trans*-NHs are generally the most favored (**Figure 1.12**). Substitution at the porphyrin periphery or at the inner nitrogen atoms can induce a preferred *trans*-NHs delocalization pathway which is often a determinant of chemical reactivity. The less favored *cis*-NH tautomers are believed to be intermediates in a stepwise N-H migration mechanism [26].

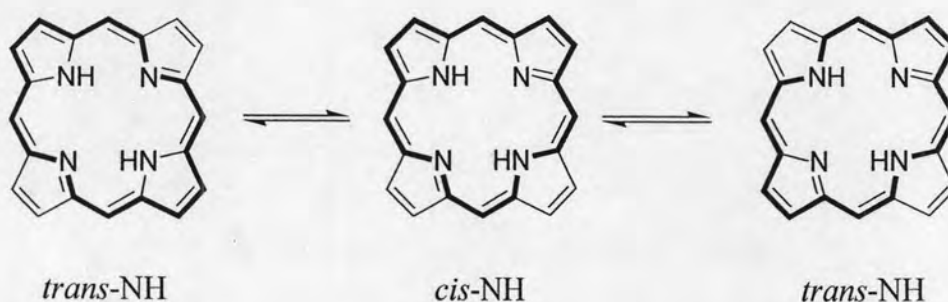


**Figure 1.12** The conjugation pathway in the [18]-annulene structure of porphyrins

Generally, the electronically most reactive sites at the periphery of porphyrins are the *meso*-positions which are sterically less accessible when one or two of the abutting  $\beta$ -positions are substituted. In contrast, the  $\beta$ -positions are usually sterically less congested, and are the preferential reaction sites of porphyrins in the presence of bulky reactant species.

### 1.4.1 Electrophilic Reactions

The most common reactions of porphyrins and their derivatives are electrophilic substitutions. Metallation of the inner core of porphyrins prevents the formation of non-nucleophilic deactivated  $N,N'$ -diprotonated species. Porphyrins undergo halogenation at the peripheral unsubstituted *meso*- and  $\beta$ -positions. Fluorination and chlorination are favored at the most reactive *meso*-positions [27-28]. Bromination occurs readily at both the *meso*- and  $\beta$ -positions by using NBS as shown in **Figure 1.13** [29-30], whereas iodination takes place mainly at the more sterically accessible  $\beta$ -positions [31]. Bromoporphyrins are useful materials in the formation of substituted porphyrins *via* the cross-coupling reactions.

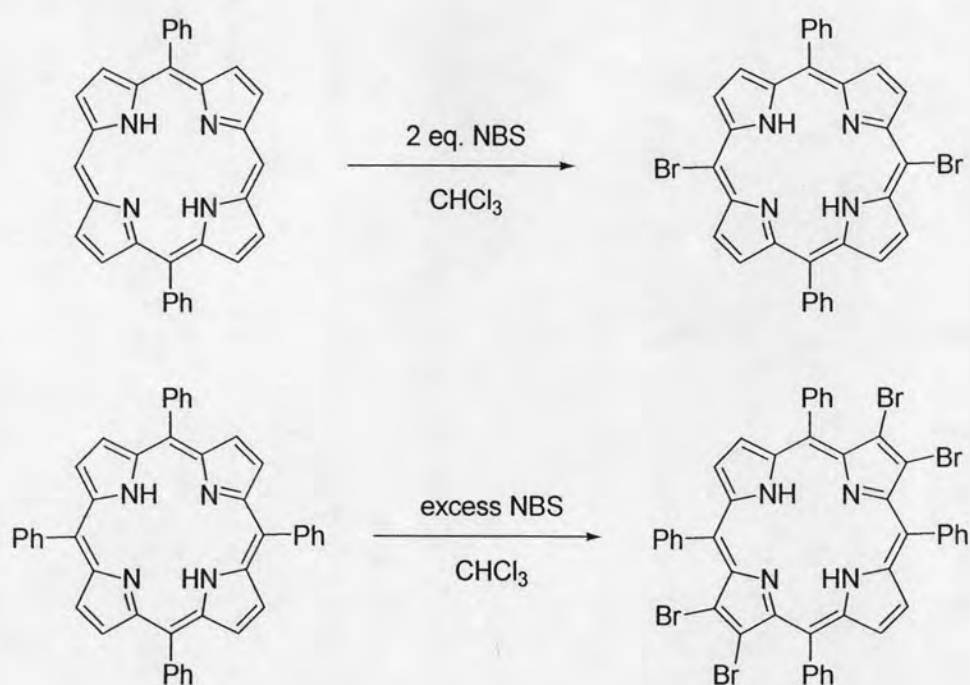


**Figure 1.13** Bromination of porphyrins by using NBS [29-30]

In addition to halogenation, several types of electrophilic reactions of porphyrin derivatives including nitration, formylation, acylation, mercuration, and additions of carbenes and nitrenes have been reported in many literatures [32].

### 1.4.2 Nucleophilic Reactions

Porphyrins can be attacked by nucleophiles, such as organometallic reagents, preferentially at the *meso*-positions, with the formation of phlorins and



porphodimethanes, or less commonly at the  $\beta$ -positions, with the formation of chlorins. The basic structures of phlorins, porphodimethanes, and chlorins are illustrated in **Figure 1.14**. The best known nucleophilic addition reactions occur on the  $\pi$ -cation radicals of metalloporphyrins, which can be obtained by chemical or electrochemical oxidation [33].

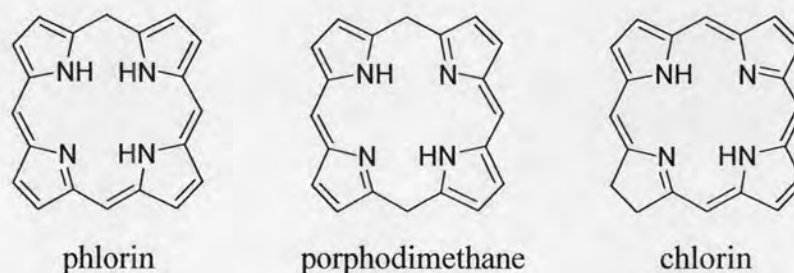


**Figure 1.14** The basic structures of phlorins, porphodimethanes, and chlorins

### 1.4.3 Reductions, Oxidations, and Other Reactions

Reductions [34] and oxidations [35] are amongst the better studied reactions of porphyrins and lead to a variety of interesting new porphyrin derivatives with characteristic chemical and physical properties. Porphyrins can be reduced to a variety of dihydro- (chlorins, phlorins, porphodimethanes), tetrahydro- (isobacteriochlorins, bacteriochlorins, porphomethanes), and hexahydroporphyrins (porphyrinogens) and oxidized to afford, for example, oxophlorins and oxochlorins.

Other reactions such as cycloadditions, intermolecular cyclizations, rearrangements, and dimerization also generate new porphyrin systems [32], many of which bear extended  $\pi$ -conjugated systems and extraordinary chemical and physical properties.

### 1.4.4 Metallations

The porphyrin nucleus is a tetradentate ligand in which the space available for a coordinated metal has a maximum diameter of approximately 3.7 Å [36]. When the coordination occurs, two protons are removed from the pyrrole nitrogen atoms, leaving two negative charges. The porphyrin complexes with transition metal ions are very stable, for instance, the stability constant for the zinc complex of tetraphenylporphyrin is about  $10^{29}$  [36].

Almost all metal ions form 1:1 complexes, although Na, K, Li complexes are 2:1 in which the metal ions are incorporated slightly below and above the porphyrin macrocycle plane. When the divalent metal ions such as Co(II), Ni(II), and Cu(II) are chelated, the resulting tetracoordinated porphyrin complexes have no residual charge. As a result, Cu(II) and Ni(II) in their porphyrin complexes exhibit generally low affinity for additional ligands. In contrast, the porphyrins coordinated with Mg(II), Cd(II) and Zn(II) readily combine with one more ligand to form pentacoordinated complexes with square-pyramidal structure. In addition, some porphyrin metal complexes coordinated with Fe(II), Co(II), and Mn(II) are able to form distorted octahedral structure with two extra ligand molecules [37].

The reactions in which the insertions of the metal ions into the inner core of porphyrins occur are usually followed by UV-visible absorption spectroscopy. Metallations of porphyrins can be done in various conditions of solvents with specific methods [38] described as follows.

#### **1.4.4.1 Chloroform/Methanol Method**

A refluxing concentrated chloroform solution of porphyrins is treated with a saturated solution of the metal(II) acetate. After completion reaction, the mixture is concentrated and diluted with methanol to give the metalloporphyrins usually in near quantitative yield. Tetrahydrofuran can be used instead of chloroform because of good solubility and low boiling point which reduce the chance of thermal decomposition of sensitive substituents on porphyrins.

#### **1.4.4.2 Dimethylformamide Method**

Dimethylformamide (DMF) is a uniformly good solvent for both porphyrins and metal salts, usually metal chloride. The HCl produced in the reaction escapes at the reflux temperature of the solvent. This is the method of choice for phenyl- and/or pyrrole substituted *meso*-porphyrins primarily due to their insolubility in lower boiling solvents and also their higher thermal stability. The products are crystallized by dilute water or dilute HCl to dissolve the excess metal salts in the reaction mixture. A major disadvantage of DMF is that it can decompose to give dimethylamine which will neutralize HCl produced in the reaction and can lead to complicating side reactions, if long reaction times are required. This is particularly so in the case of

highly electron deficient halogenated porphyrin systems where DMF may act as a nucleophile leading either to halogen substitution or to porphyrin destruction.

#### **1.4.4.3 Acetic acid/Acetate Method**

In this method, metal acetate salts are heated with porphyrins in acetic acid at 100 °C. The products are crystallized either directly by cooling or by the addition of water or methanol. In the case of oxidizable metals with multi-oxidation state such as Mn(II) and Fe(II), the complex can be autooxidized to the more stable high oxidation state.

#### **1.4.4.4 Pyridine Method**

This is a useful method for metalloporphyrins labile toward acetic acid since pyridine is a good solvent for porphyrins and metal salts. Pyridine forms complexes with metals of high charge and consequently retards the metallation process.

#### **1.4.4.5 Metal Carbonyl Method**

This method has been proven to be especially useful for the preparation of metalloporphyrins of VI-VIII metal groups. The metal carbonyl or the carbonyl chloride is heated with porphyrins in inert solvent such as benzene, toluene, or decalin.

#### **1.4.4.6 Acetylacetonone Method**

Metal acetylacetonates make very useful carries due to their availability, solubility in organic solvents at the low  $pK_a$  of the acid liberated during the reaction. With the metal ions of high charge and small size, a weakly acidic solvent, such as phenol, is required to liberate the active metallating species. This method has been used with IIIA and IIIB metal groups.

### **1.4.5 Demetallations**

The demetallation processes can be done to remove the metal ions from the complexes. Demetallations are favored by the presence of acid since protonation of free base drives the equilibrium in the forward direction [38]. The stability of

metalloporphyrins is often defined in terms of the degree of resistance to the displacement of the metal atoms by acid. Several stability classes have been identified based on the degree of completeness of the demetallations in acetic acid, aqueous HCl-dichloromethane, and sulfuric acid. Some divalent metal ions, such as Zn(II), are readily removed by trifluoroacetic acid in dichloromethane, while Cu(II) requires 15-20% of sulfuric acid in trifluoroacetic acid or sometimes even stronger conditions.

### 1.5 Photophysical Properties of Porphyrins

On account of the large  $\pi$ -conjugated systems of porphyrins and their related derivatives, these macrocyclic compounds display interesting and extraordinary photophysical properties, especially as shown in their UV-visible absorption and fluorescence emission spectra.

Typically, the electronic absorption spectrum of a simple porphyrin, such as octaethylporphyrinatozinc(II) (ZnOEP) consists of a strong transition to the second excited state ( $S_0 \rightarrow S_2$ ) at about 400 nm called the Soret or B band and a weak transition to the first excited state ( $S_0 \rightarrow S_1$ ) at around 500-700 nm called the Q band. The Soret band and Q band both arise from  $\pi$ - $\pi^*$  transitions and can be explained by considering the four frontier orbitals (the "Gouterman's four orbital model", as shown in **Figure 1.15**): two  $\pi$  orbitals ( $a_{1u}$  and  $a_{2u}$ ) and a degenerate pair of  $\pi^*$  orbitals ( $e_{gx}$  and  $e_{gy}$ ). The two highest occupied  $\pi$  orbitals happen to have about the same energy. One might imagine that this would lead to two almost coincident absorption bands due to  $a_{1u} \rightarrow e_g$  and  $a_{2u} \rightarrow e_g$  transitions, but in fact these two transitions mix together by a process known as configurational interaction, resulting in two bands with very different intensities and wavelengths. The constructive interference leads to the intense short-wavelength Soret band, while the weak long-wavelength Q band results from destructive combinations. The two types of position on the porphyrin periphery are referred to as *meso*- and  $\beta$ -positions. The  $a_{1u}$  orbital has nodes at all four *meso*-positions whereas the  $a_{2u}$  orbital has high coefficients at these sites [39].



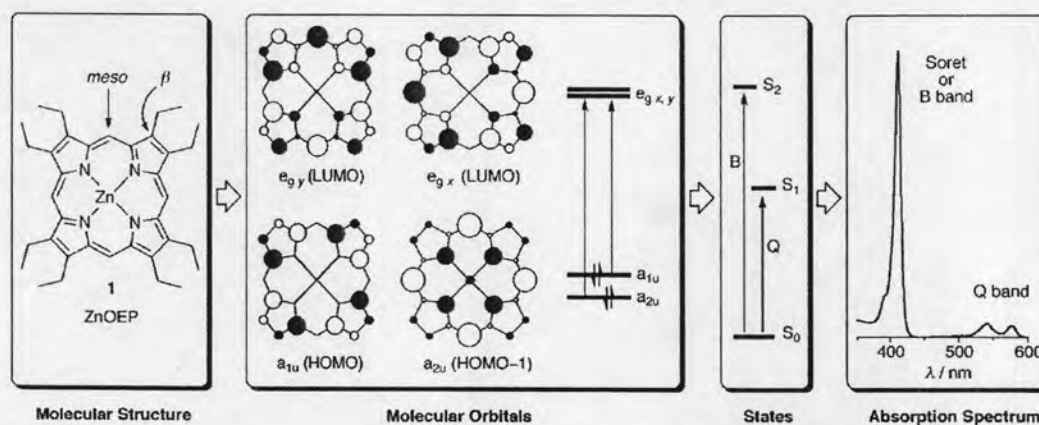


**Figure 1.15** The Gouterman's four orbital model and the electronic absorption spectrum of a simple porphyrin [39]

For the fluorescence emission, an energy level diagram that describes the emission from most aromatic molecules with singlet ground state [40] is exhibited in **Figure 1.16**. Excitation from the ground state  $S_0$  to any singlet excited state  $S_x$  leads to very fast radiationless decay to the first excited singlet state  $S_1$ . From the first excited singlet state  $S_1$ , the molecule can emit fluorescence radiation  $S_1 \rightarrow S_0$  at the rate  $k_f$ , can radiationlessly decay  $S_1 \rightarrow S_0$  at the rate  $k_1$ , or can internally convert to the first triplet  $S_1 \rightarrow T_1$  at the rate  $k_2$ . The first excited singlet state  $S_1$  decays between  $10^{-12}$  and  $10^{-7}$  s, after which, if the system is still excited, it exists in the first triplet state  $T_1$ . From the first triplet state  $T_1$ , the molecule can emit phosphorescence radiation  $T_1 \rightarrow S_0$  at the rate  $k_p$ , can radiationlessly decay  $T_1 \rightarrow S_0$  at the rate  $k_3$ , or can be excited again to the first excited singlet state  $T_1 \rightarrow S_1$  at the rate  $k_2$ . Therefore, only the relaxation process from  $S_1$  to  $S_0$  with rate  $k_f$  can emit fluorescence radiation. In the case of porphyrins, the internal conversion from the second excited state to the first excited state ( $S_2 \rightarrow S_1$ ) is rapid; hence, fluorescence is only detected from the first excited state  $S_1$  [39].

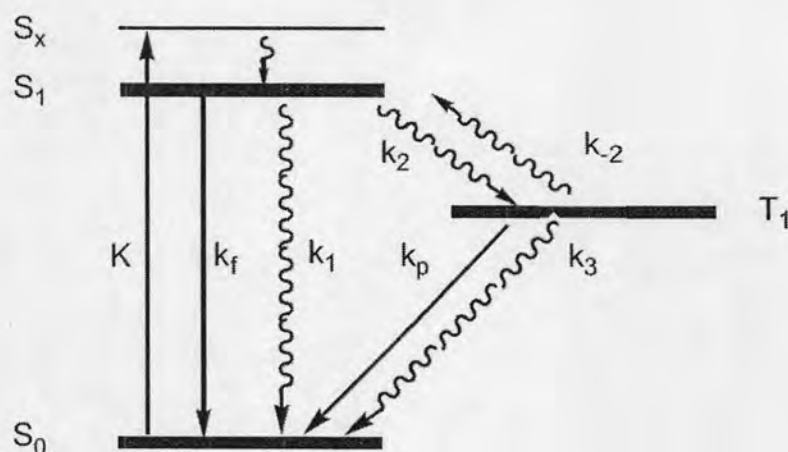


**Figure 1.16** The energy level diagram to explain the fluorescence emission [40]

### 1.6 Conjugate-Linked Porphyrins

Porphyrins are tetrapyrrolic conjugated systems which have a small energy gap between the highest occupied molecular orbital (HOMO) and the lowest unoccupied molecular orbital (LUMO) as compared with the other molecules that are used as materials in the optoelectronic devices. As a result, this class of molecules has been intensively studied in points of molecular design, synthetic strategy, property modification, and fabrication process. In order to develop the new organic functional materials supporting the present optoelectronic society life, the extended  $\pi$ -electronic conjugated systems of porphyrin nuclei connecting with various linkers have been vastly demonstrated, by virtue of their high susceptibilities to the optical and electronic stimulations [41]. Especially at the molecular design for functional materials, it is very important to choose a particular one from various linkers which can construct the electronic structure of the molecule both purposively and precisely. For example, the intensification of particular bands participating in a material functionality in the electronic absorption spectra would lead to an enhancement of their responses and sensing capabilities to the outside stimulations. In addition to such an auxiliary modification of the main electronic structure, the extension of  $\pi$ -conjugated system would make an electronic activation of the molecule much easier, leading to the wider versatility of photo-sensing functionalities such as nonlinear optical (NLO) phenomena and to the further processibility for the material devices as well [42].

As mentioned above, several conjugated linkers including phenyl, aryl, alkene, imine, alkyne, and azo functional groups are interesting candidates to extend the  $\pi$ -conjugated system of porphyrins by connecting these linkers directly to the porphyrin ring at the *meso*- or  $\beta$ -positions. The nature and position of the linkers can have a strong influence on the overall properties of porphyrins. In recent years, a number of conjugate-linked porphyrin derivatives has been synthesized and investigated of their properties.

Most of synthetic porphyrins have aryl substituents at the *meso*-positions. These cause only a slight perturbation to the electronic structure because of the minimal  $\pi$ -overlap between the aryl ring and the porphyrin ring which results from steric interactions with the  $\beta$ -hydrogens or  $\beta$ -substituents of porphyrins. Due to this non-planarity, *meso*-aryl-linked porphyrins do not exhibit significant conjugation [43]. Similarly, *meso*-phenylene-linked porphyrin and directly *meso-meso* bonded porphyrin oligomers are not conjugated for the same reason (**Figure 1.17**) [44]. As a result, their absorption spectra show almost identical to those of the corresponding unsubstituted porphyrins [45].

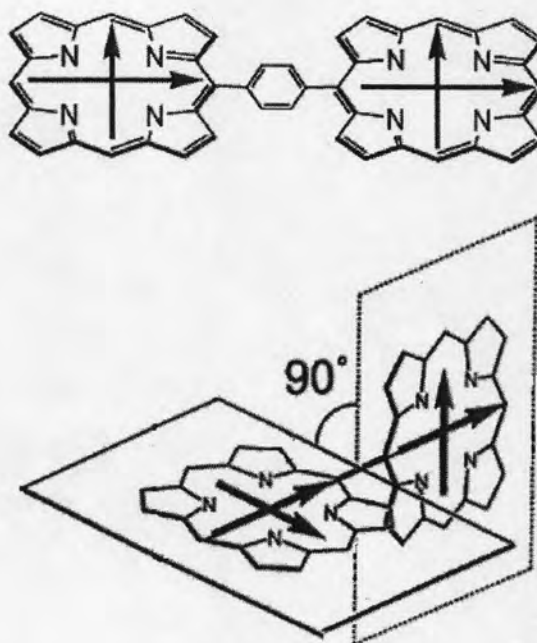


**Figure 1.17** Structures of *meso*-phenylene-linked porphyrin and directly *meso-meso* bonded porphyrin oligomers

In 2002, Screen and co-workers reported the synthesis of a series of porphyrins in which an aryl substituent was linked to the porphyrin *via* azo, imine, alkene, and alkyne bridges (**Figure 1.18**) [46]. The strength of porphyrin-aryl conjugation was assessed by comparing the absorption and emission spectra of these compounds, and by crystallographic and computational analysis of their geometries. The planarity was evaluated by measuring the torsional angles between the mean planes of porphyrin ring and the linker ( $\theta_{AB}$ ) and between the planes of the linker and the phenyl ring ( $\theta_{BC}$ ) as illustrated in **Figure 1.19**.

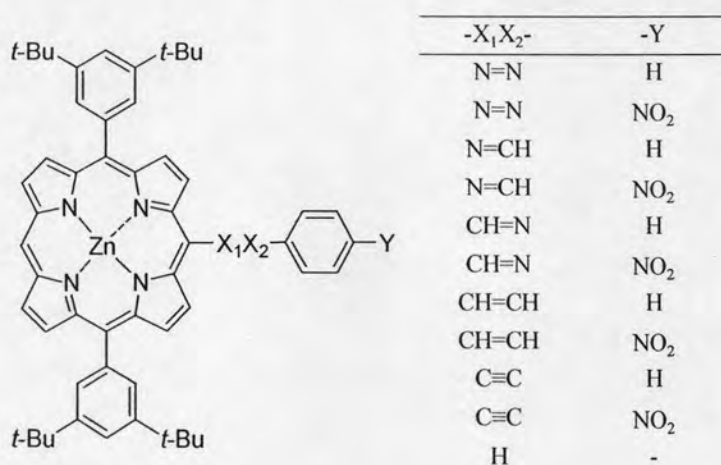


**Figure 1.18** Structures of *meso*-substituted porphyrins with conjugated linkers

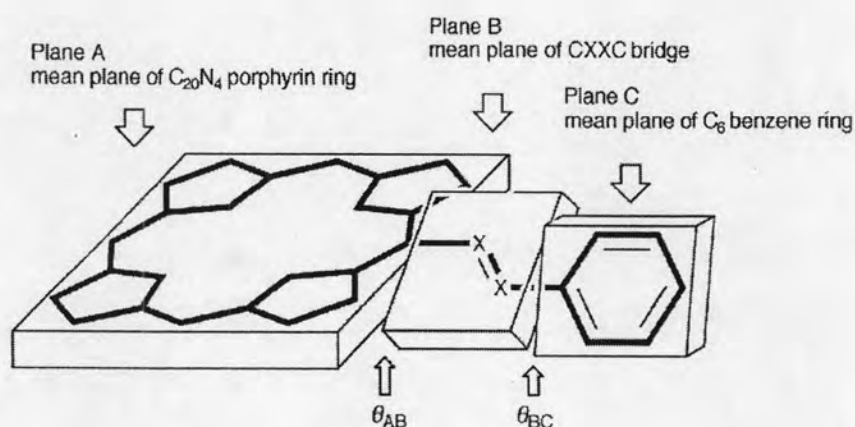


**Figure 1.19** Model of the definition of torsional angles  $\theta_{AB}$  and  $\theta_{BC}$  [46]

Analysis of the electronic spectra of porphyrin-aryl compounds showed that the azo- and alkyne-linked porphyrins allowed strong efficient  $\pi$ -overlap between the porphyrin and the aryl moiety. This was manifested by strong red shifts in the absorption and emission spectra relative to the other porphyrins, a large increase in



oscillator strength of the Q band and a further red shift and intensification of the Q band on addition of a nitro group. Moreover, the strong electronic communication could be confirmed by the X-ray crystal structure which showed almost coplanar between the porphyrin macrocycle and the linker. In contrast, alkene- and imine-linked porphyrins did not provide a good conjugation because their crystal structures showed a large twist across the bridging unit. Imine- and alkyne-linked porphyrin dimers were also synthesized; the alkyne-linked dimer is much more conjugated than its imine-linked analogue.

These results suggested that alkyne groups are interesting linkers to extend the  $\pi$ -conjugated system of porphyrins and alkyne-linked porphyrins may be potential as optoelectronic materials.

### 1.7 Alkyne-Linked Porphyrins

In general, alkyne-linked porphyrins can be synthesized by a Sonogashira coupling which is a coupling reaction of terminal alkynes with aryl or vinyl halides. Typically, two catalysts are needed for this reaction: a zerovalent palladium complex and a halide salt of copper(I). The reaction mechanism revolves around two cycles including a palladium cycle and a copper cycle as shown in **Figure 1.20**. The phosphine-palladium complexes such as tetrakis(triphenylphosphine)palladium(0) are commonly used to activate the organic halides by oxidative addition into the carbon-halogen bond. However, palladium(II) complexes such as bis(triphenylphosphine)palladium(II) chloride are also available in this reaction because they can be reduced to the palladium(0) species by the consumption of terminal alkynes and the oxidation of triphenylphosphine to triphenylphosphine oxide can also lead to the formation of palladium(0) *in situ*. In the other side, copper(I) halides react with the terminal alkyne and produce copper(I) acetylide, which acts as an activated species for the coupling reaction. Importantly, the reaction medium must be basic in order to neutralize the hydrogen halide produced as the byproduct, so alkylamine compounds such as diethylamine, triethylamine, and diisopropylamine are sometimes used.

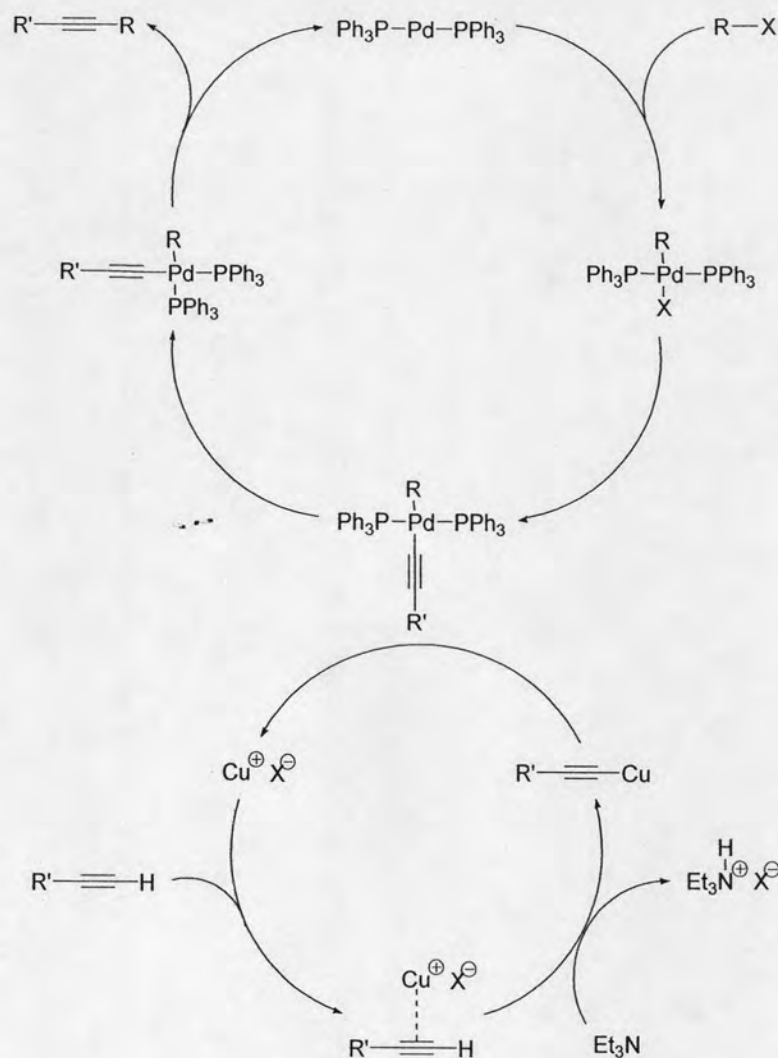


**Figure 1.20** The mechanism of Sonogashira coupling reaction

Due to the demonstration that organic molecules with extended  $\pi$ -conjugated bridges connected with electron donors and acceptors can exhibit outstanding optical properties, some functionalized alkyne-linked porphyrins were investigated.

In 2002, Plater and co-workers presented the preparation of some new donor-acceptor porphyrins based on a metallated diethynylporphyrin core [47]. These porphyrins possess 4-dimethylaminophenyl as the electron donor group and 4-nitrophenyl, 4-cyanophenyl, and 5-nitrothiazoyl as the electron acceptor group (**Figure 1.21**). Porphyrins containing the 4-nitrophenyl and 4-cyanophenyl acceptor group showed similar long wavelength absorption at 679 and 675 nm, respectively, while porphyrins containing the 5-nitrothiazoyl acceptor group showed red shifted long wavelength absorption at 766 nm.

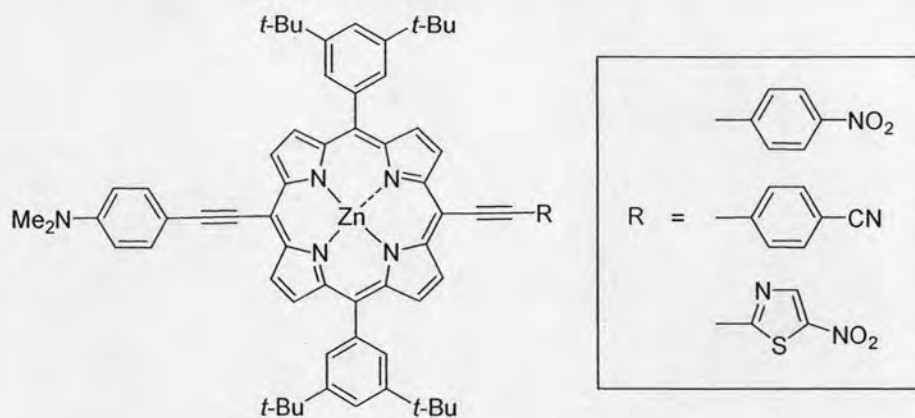


**Figure 1.21** Structures of porphyrins containing 4-dimethylaminophenyl as the electron donor group and 4-nitrophenyl, 4-cyanophenyl, and 5-nitrothiazoyl as the electron acceptor group

In 2004, Cheng and co-workers have employed the Sonogashira coupling reactions to prepare a series of *meso*-ferrocenylethynyl 5,15-diphenylporphyrins (**Figure 1.22**) [48]. Three of these compounds contain electron withdrawing groups including -CHO, -CH=C(CN)<sub>2</sub>, and -C≡CC<sub>6</sub>H<sub>4</sub>NO<sub>2</sub> at the remaining *meso*-positions, in which ferrocene serves as the electron donor group. All of ferrocenyl porphyrin nickel complexes showed typical absorptions, giving a strong Soret band at 434-459 nm and one to two Q bands at 560-570 and 621-649 nm which were significantly red shifted compared to those of (5,15-diphenylporphyrinato)nickel(II). However, the absorption bands of ferrocenylethynyl porphyrins appeared at shorter wavelength compared to that of the 4-dimethylaminophenylethynyl porphyrins. These observations indicated that the ferrocenylethynyl group can extend the  $\pi$ -conjugation of the central porphyrin core, but the extent seems to be smaller than 4-dimethylaminophenylethynyl moiety. This was confirmed by the molecular structure of ferrocenylethynyl porphyrins from the X-ray diffraction analysis as depicted in **Figure 1.23**. The structure suggested that the cyclopentadienyl rings of ferrocene are non-coplanar with the porphyrin core. Another remarkable feature of the absorption spectra of these ferrocenyl porphyrins is the broadening of signals, which may suggest a partial mixing of  $\pi$ - $\pi^*$  transition with an intramolecular charge transfer character.

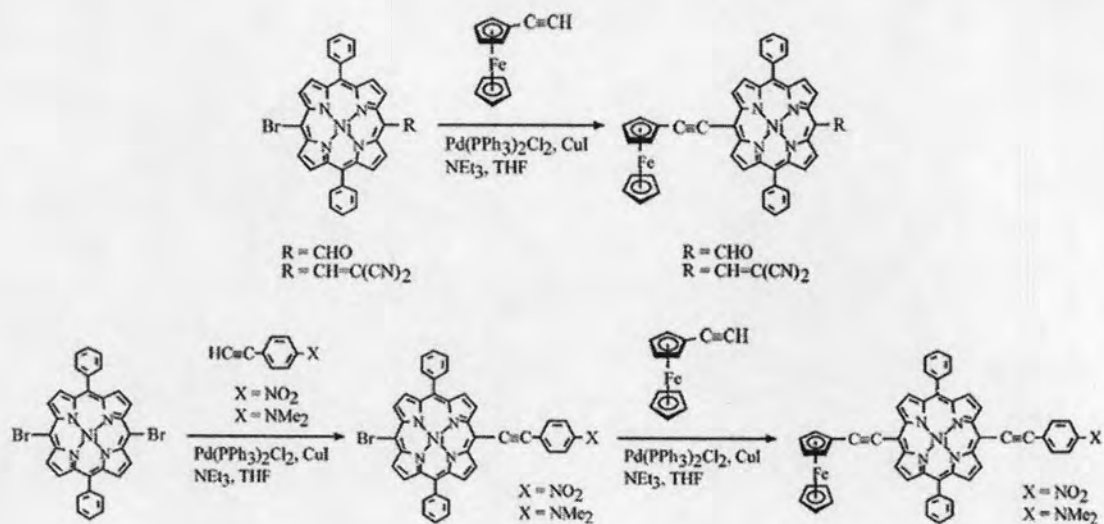


**Figure 1.22** Synthesis of *meso*-ferrocenylethynyl porphyrins

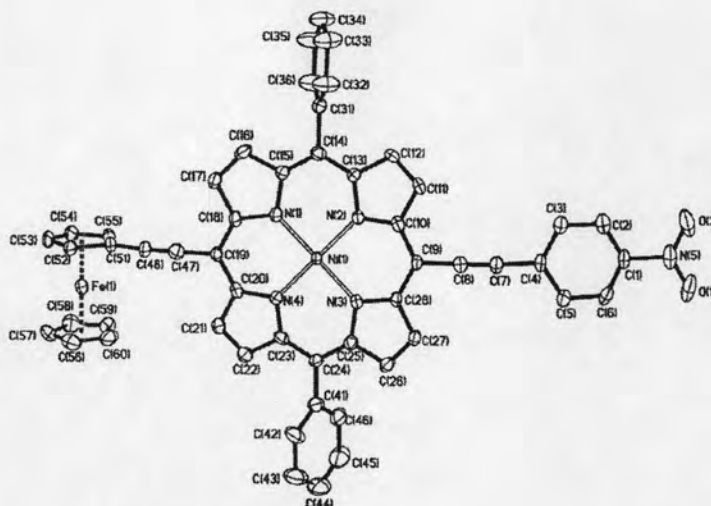


**Figure 1.23** The molecular structure of *meso*-ferrocenylethynyl porphyrin from the X-ray diffraction analysis

In 2005, Zhang and co-workers have synthesized an extensive series of conjugated (porphyrinato)zinc(II)-based chromophores featuring nitrothiophenyl and nitrooligothiophenyl electron-accepting moieties using metal-catalyzed cross-coupling reactions [49]. From **Figure 1.24**, the absorption bands of donor-acceptor porphyrin exhibited red shifts relative to those of corresponding porphyrin and oligothiophene. This indicated the extension of  $\pi$ -conjugation and strong electronic communication between the donor and acceptor moieties. Nonlinear optical properties



of these porphyrins have been also investigated. The data indicated that these neutral dipolar asymmetric porphyrin-thiophene chromophores may thus find utility for optoelectronic applications at telecom-relevant wavelengths.

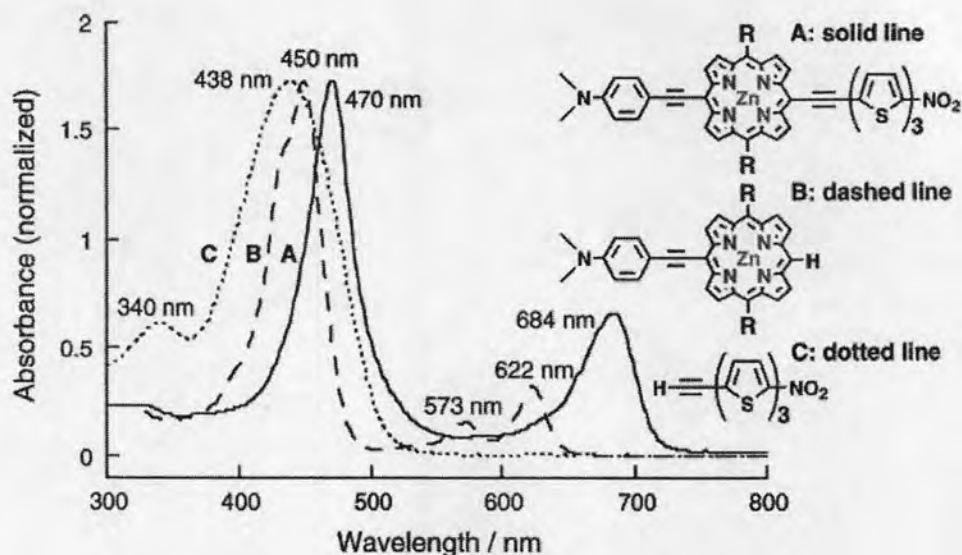


**Figure 1.24** The absorption spectra of donor-acceptor porphyrin and its corresponding compounds

Moreover, Zhang and co-workers also reported the synthesis of a series of conjugated (porphyrinato)zinc(II)-based chromophores structurally related to compound 1 in **Figure 1.25** via cross-coupling reactions involving brominated porphyrins or terminal ethyne derivatives of porphyrins along with appropriately functionalized aryl, thienyl (or thiophenyl), thiazolyl, benzothiazolyl, and carbazolyl precursors [50]. The linear and nonlinear optical properties of these asymmetrically 5,15-substituted-(10,20-diarylporphyrinato)zinc(II) chromophores that bear an electron-donating group and an electron-withdrawing group (**Figure 1.25**) were studied. The dynamic hyperpolarizabilities of these compounds were determined from hyper-Rayleigh light scattering measurements carried out at a fundamental incident irradiation wavelength of 1300 nm. These data highlight that reductions in the magnitude of the aromatic stabilization energy of (porphyrinato)metal-pendant arylethynyl groups have a significant impact upon the magnitude of the molecular hyperpolarizability and provide insights into advantageous design modifications for closely related structures having potential utility in long-wavelength optoelectronic applications.

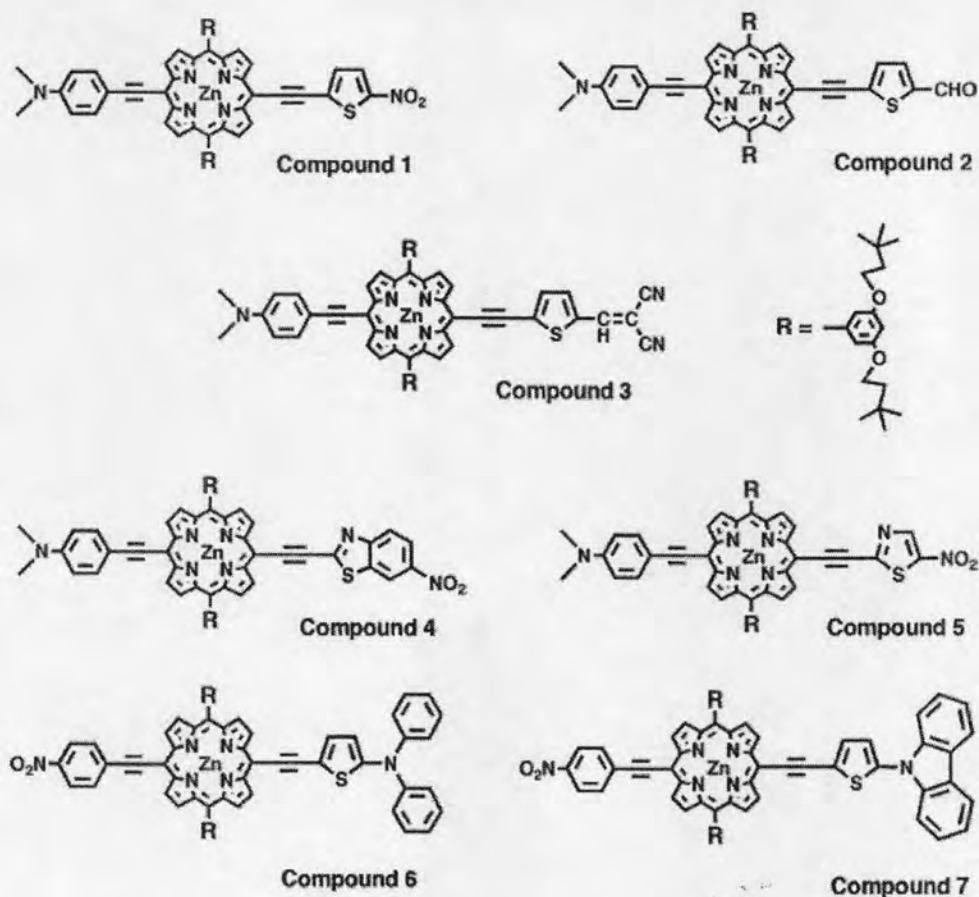


**Figure 1.25** Structures of asymmetrically 5,15-substituted-(10,20-diarylporphyrinato)zinc(II) chromophores

In 2009, the synthesis and electrochemical and photophysical investigations of new electron donor-acceptor arrays, bearing porphyrins covalently linked to fullerene, were described by Lembo and co-workers [51]. Ethynylene phenylene subunits were chosen as a linking bridge to guarantee a high conjugation degree between the donor (*i.e.*, porphyrin), the molecular bridge, and the acceptor (*i.e.*, fullerene) as illustrated in **Figure 1.26**. To enhance the electronic interactions through the extended  $\pi$ -system, the molecular bridge has been directly linked to the  $\beta$ -pyrrole position of the porphyrin ring, generating a new example of donor-bridge-acceptor systems. This modification allowed alteration of the chemical and physical properties of porphyrin ring. Absorption and fluorescence measurements revealed that in nonpolar media transduction of singlet excited-state energy governed the excited-state deactivation, whereas in polar media charge transfer prevailed generating a long-lived radical ion pair state. The study also underlined the wirelike behavior of the linker on the donor features. Photophysical and electrochemical studies implied that the conformation of

the porphyrin relative to the phenyl rings of the bridge prevented the full conjugation between donor and the linker. The mechanism of the charge-transfer processes seems to remarkably depend on the structural properties of the linker between donor and acceptor and its conjugation into the porphyrin/fullerene moieties. These findings have been corroborated by local electron affinity mappings.

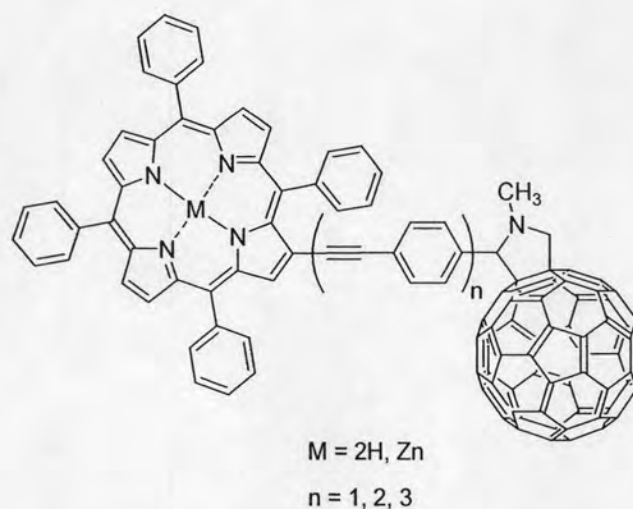


**Figure 1.26** Structures of porphyrin-fullerene with ethynylene-phenylene subunits

In order to examine the effect of the position of alkyne linkers on the  $\pi$ -conjugation of porphyrins, *meso-meso*, *meso- $\beta$* , and  *$\beta$ - $\beta$*  porphyrin dimers were studied by Lin and Therien (**Figure 1.27**) [52]. The results showed that *meso-meso* connectivity conferred maximum electronic coupling, whereas *meso- $\beta$*  and  *$\beta$ - $\beta$*  connectivity exhibited weak electronic communication. The poor conjugation in the *meso- $\beta$*  and  *$\beta$ - $\beta$*  ethyne-linked dimers can be attributed to steric clashes, forcing the molecules into orthogonal conformations, and may be due to the smaller frontier orbital coefficients at the  $\beta$ -positions.

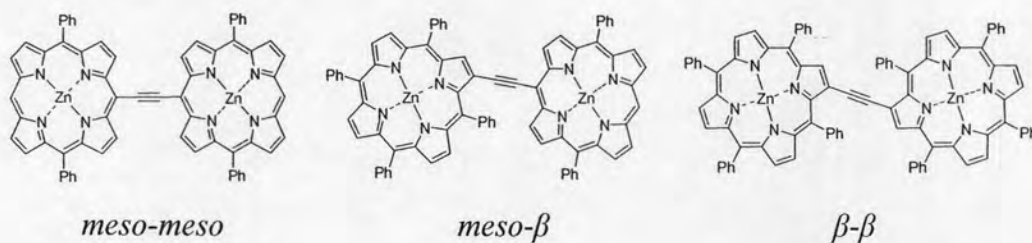


**Figure 1.27** Structures of *meso-meso*, *meso- $\beta$* , and  *$\beta$ - $\beta$*  ethyne-linked porphyrin dimers

## 1.8 Objectives

This research is aimed to synthesize an extensive series of *meso*-alkyne-linked porphyrin metal complexes. The general structure of these porphyrins is illustrated in **Figure 1.28**. All of the synthesized porphyrins will be characterized by  $^1\text{H}$  NMR spectroscopy and MALDI-TOF mass spectrometry. Moreover, UV-visible absorption spectroscopy and fluorescence spectroscopy are also used to investigate their photophysical properties. Effects of metal ions as well as various substituents of synthesized porphyrins on photophysical properties will be discussed. Finally, coordination properties of synthesized porphyrins will be preliminarily studied by  $^1\text{H}$  NMR, UV-visible, and fluorescence spectroscopic titration.

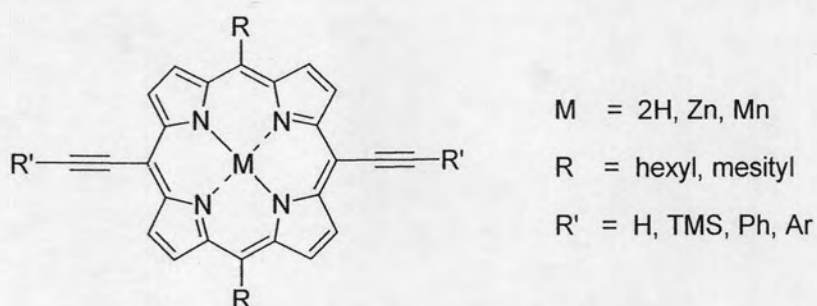


**Figure 1.28** The general structure of target porphyrins